Interspecies comparison of metabolism of two novel prototype PFAS

Licul-Kucera, V.; Ragnarsdóttir, O.; Frömel, T.; van Wezel, A.P.; Knepper, T.P.; Harrad, S.; Abou-Elwafa Abdallah, M.

DOI
10.1016/j.chemosphere.2024.141237

Publication date
2024

Document Version
Final published version

Published in
Chemosphere

License
CC BY

Chemosphere 351 (2024) 141237

Contents lists available at ScienceDirect

Chemosphere

journal homepage: www.elsevier.com/locate/chemosphere

Interspecies comparison of metabolism of two novel prototype PFAS

Viktória Licul-Kucera [a,b,*], Oddný Ragnarsdóttir [c], Tobias Frömel [b], Annemarie P. van Wezel [a], Thomas P. Knepper [b], Stuart Harrad [c], Mohamed Abou-Elwafa Abdallah [c]

[a] Institute for Biodiversity and Ecosystem Dynamics, University of Amsterdam, Amsterdam, Netherlands
[b] Institute for Analytical Research, Hochschulen Fresenius Gem. Trägergesellschaft MbH, Idstein, Germany
[c] School of Geography, Earth & Environmental Sciences, University of Birmingham, Birmingham, UK

HIGHLIGHTS

- Novel prototype chemicals were designed as alternatives to current PFAS.
- Slow metabolism was observed by human and rat S9 fractions.
- Main metabolites were alcohols and carboxylic acids with ≤3 fluorinated carbons.
- Metabolism was faster in rat than in human.
- *S*-linkage prototypes were metabolized faster than those with O-linkage.

GRAPHICAL ABSTRACT

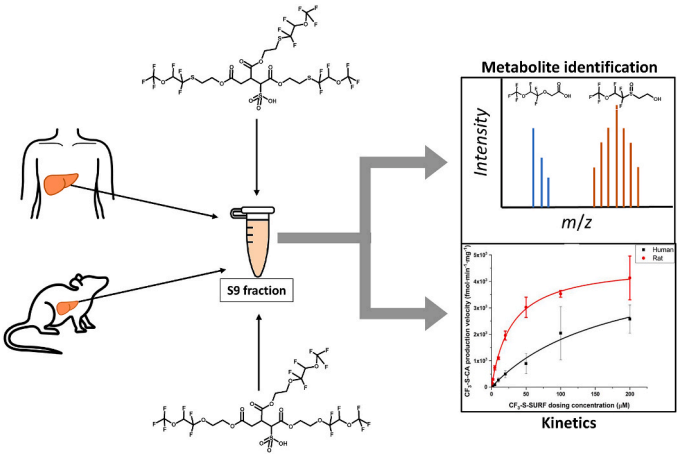

ARTICLE INFO

Handling editor: Giulia GUERRIERO

Keywords:
PFAS
Alternative chemicals
In vitro metabolism
Liver S9
Human
Rat

ABSTRACT

As a result of proposed global restrictions and regulations on current-use per-and polyfluoroalkyl substances (PFAS), research on possible alternatives is highly required. In this study, phase I *in vitro* metabolism of two novel prototype PFAS in human and rat was investigated. These prototype chemicals are intended to be safer-by-design and expected to mineralize completely, and thus be less persistent in the environment compared to the PFAS available on the market. Following incubation with rat liver S9 (RL-S9) fractions, two main metabolites per initial substance were produced, namely an alcohol and a short-chain carboxylic acid. While with human liver S9 (HL-S9) fractions, only the short-chain carboxylic acid was detected. Beyond these major metabolites, two and five additional metabolites were identified at very low levels by non-targeted screening for the ether- and thioether-linked prototype chemicals, respectively. Overall, complete mineralization during the *in vitro* hepatic metabolism of these novel PFAS by HL-S9 and RL-S9 fractions was not observed. The reaction kinetics of the surfactants was determined by using the metabolite formation, rather than the substrate depletion approach. With rat liver enzymes, the formation rates of primary metabolite alcohols were at least two orders of magnitude

* Corresponding author.Institute for Biodiversity and Ecosystem Dynamics, University of Amsterdam, Amsterdam, Netherlands
E-mail address: v.liculkucera@uva.nl (V. Licul-Kucera).

https://doi.org/10.1016/j.chemosphere.2024.141237
Received 18 October 2023; Received in revised form 11 January 2024; Accepted 15 January 2024
Available online 17 January 2024

higher than those of secondary metabolite carboxylic acids. When incubating with human liver enzymes, the formation rates of single metabolite carboxylic acids, were similar or smaller than those experienced in rat. It also indicates that the overall metabolic rate and clearance of surfactants are significantly higher in rat liver than in human liver. The maximum formation rate of the thioether congener exceeded 10-fold that of the ether in humans but were similar in rats. Overall, the results suggest that metabolism of the prototype chemicals followed a similar trend to those reported in studies of fluorotelomer alcohols.

1. Introduction

Per- and polyfluoroalkyl substances (PFAS) are a diverse group of synthetic chemicals widely used in many industrial and consumer applications as processing aids, e.g., emulsifiers, surfactant, lubricants, water-and oil repellents, inert media (Glüge et al., 2020). PFAS have received increasing attention in the last years as studies have shown their ubiquitous distribution in the environment (Björnsdotter et al., 2021; Coggan et al., 2019; Cousins et al., 2022; González-Barreiro et al., 2006; Gremmel et al., 2017; Janousek et al., 2019). This stems from their physicochemical properties namely, high persistence (vP) and either high bioaccumulation potential (vB) or high mobility (vM). These properties both carry a level of concern for human exposure through the food chain or drinking water respectively (Hale et al., 2020). Significant health effects of PFAS have been suggested by several studies linking PFAS exposure to hepatic (Salihovic et al., 2018; Sen et al., 2022), renal (Stanifer et al., 2018) and thyroid dysfunction (Preston et al., 2021), preterm birth (Gardener et al., 2021) and immunotoxicity (Grandjean et al., 2017; DeWitt et al., 2019).

Based on the abovementioned risks, several jurisdictions have implemented restrictions on the use of certain PFAS over the past twenty years, e.g., under the Stockholm Convention (United Nations Environment Programme, 2009, United Nations Environment Programme, 2019, United Nations Environment Programme, 2022) or REACH (Registration, Evaluation, Authorisation and Restriction of Chemicals) (European Chemical Agency, 2019; European Chemical Agency, 2022; European Chemical Agency, 2020; European Commission, 2021). However, they mostly cover legacy PFAS – perfluoroalkyl carboxylic acids (PFCAs) and perfluoroalkane sulfonic acids (PFSAs) – which contain 4 to 14 carbon atoms in the chain. ECHA proposed a major legislative step towards the phase-out of all PFAS which fulfil the definition of Organisation for Economic Co-operation and Development and (OECD) for PFAS, namely "[…] that contain at least one fully fluorinated methyl (CF_3-) or methylene (-CF_2-) carbon atom (without any H/Cl/Br/I attached to it)" (Federal Institute for and Occupational Safety and Health, National Institute for Public Health and the Environment, Swedish Chemicals Agency, Norwegian Environment Agency, 2023; OECD, 2021). However, some PFAS which fulfil this definition, are excluded as they are fully degradable (Federal Institute for and Occupational Safety and Health, National Institute for Public Health and the Environment, Swedish Chemicals Agency, Norwegian Environment Agency, 2023).

According to the European Chemicals Agency (ECHA), manufacturers must demonstrate that the substance does not adversely affect the environment and human health (European Chemicals Agency, 2017). Environmental fate studies – including vPvB assessment – are essential parts of the risk evaluation of any chemical intended to be released to the environment. These studies mostly include determination of the distribution amongst different environmental compartments and investigation of its microbial degradation and transformation pathway (s). While vPvB assessment is required, the use of ADME (absorption, distribution, metabolism, elimination) data is not mandatory (European Chemicals Agency, 2017). However, ADME profiling is intensively applied and obligatory in the pharmaceutical industry (Kola and Landis, 2004; Tsaioun et al., 2016). Drug development also proves that pharmacokinetic studies are essential in understanding the behaviour of a chemical in any organism, as they provide additional information about a chemical that vPvB assessment cannot. Metabolic stability assays – as part of the ADME assessment – are performed to understand the susceptibility of a chemical to undergo biotransformation in the body (Van den Eede et al., 2013).

Chemicals can be eliminated by the organism unchanged, but the vast majority undergoes enzymatic functionalization and/or conjugation reactions that facilitate their elimination and protect the organism against an accumulation of lipid-soluble compounds (Osakwe, 2016). The liver plays an essential role in the metabolism, distribution, and excretion of xenobiotics (Sen et al., 2022). Perfluoroalkyl acids (PFAAs) e.g., PFOA and PFOS are not metabolized and are poorly eliminated from the human body but are reabsorbed via the enterohepatic circulation (Cao et al., 2022; Salihovic et al., 2018). The half-lives of PFAAs in humans can range from 1 month (PFBS) up to 8.5 years (PFOS), and increase with carbon chain length (Lau et al., 2007). PFAS precursors, e.g., fluorotelomer alcohols (FTOHs) can be metabolized, with both *in vitro* and *in vivo* studies showing the metabolism of these compounds in humans and rats (Fasano et al., 2006; Martin et al., 2005; Nabb et al., 2007). Unfortunately, these compounds can then form the more persistent PFAAs, although they are considered minor metabolites (Fasano et al., 2006; Martin et al., 2005; Nabb et al., 2007). Similar trends are seen with PFAS in nature. Under normal environmental conditions, PFAAs are hardly broken down and precursor compounds that are degradable in the environment will ultimately form persistent break-down products like PFAAs (Wang et al., 2017).

In a recent study, the environmental fate of two novel PFAS surfactants with a trifluoromethoxy headgroup was investigated (Licul-Kucera et al., 2023). These chemicals, which are not yet manufactured and used commercially, are covered by the OECD PFAS definition, however, they were expected, in theory, to degrade completely, i.e., mineralize in the environment. However, the study found that while only 2.5% and 1.2% of the starting surfactant was detected after 126 days, the unequivocal final mineralization of the investigated surfactants was not observed. Therefore, it is important to assess the possible fate of these chemicals in organisms of higher trophic level prior to the final decision about their legislation. In the present study we investigate the *in vitro* phase I metabolism of these prototype PFAS surfactants in human and rat S9 subcellular fractions. We provide first insights into the *in vitro* pharmacokinetics of these novel chemicals in humans and rat and compare the differences in the rate of metabolism as well as inter-species metabolic profiles. Our aim is to understand the suitability of these novel chemicals – that are also PFAS according to both the Buck- and OECD-definition – as more environmentally-friendly alternatives to current PFAS (Buck et al., 2011; OECD, 2021; Wang et al., 2021).

2. Materials and methods

2.1. Chemicals

2.1.1. Novel prototype PFAS chemicals

The novel prototype PFAS were designed and synthesized by Merck KGaA (Darmstadt, Germany). These chemicals are in the developmental phase and not yet available on the market. They are abbreviated as CF_3-O-SURF and CF_3-S-SURF in this study. The theoretically expected transformation products (TPs), abbreviated as CF_3-O-ALC, CF_3-S-ALC, CF_3-O-CA, CF_3-S-CA and CF_3-CA were also synthesized and measured during the study. The synthesized standards of CF_3-O-SURF and CF_3-S-

SURF contained 1.3 and 3.5 w/w% impurity from CF_3-O-ALC and from CF_3-S-ALC, respectively. The structure, molecular formula and molecular weight of the prototype PFAS and their TPs are presented in Table 1. SMILES strings of them are listed in Table S1. *In silico*-based predictions of water solubility and pK_a values of parent substances are available in Table S2. More details about the molecular structure of the prototype PFAS are available in 3.1.

2.1.2. Further standards and chemicals

Perfluoropropionic acid (PFPrA), perfluoropropane sulfonic acid (PFPrS), perfluorohexanoic acid (PFHxA), perfluorononanoic acid (PFNA) and perfluorodecanoic acid (PFDA) were used as internal standards (IS). Their supplier and purity were given in Table S3. Water and methanol (MeOH) (both LiChrosolv®, ultrahigh-performance liquid chromatography−mass spectrometry (UHPLC-MS) grade) and dimethyl sulfoxide (DMSO) (≥99.7% purity) were obtained from Merck KGaA (Darmstadt, Germany). Ammonium acetate (>99% purity) was bought from Fluka (Munich, Germany). Rat liver S9 fractions (pooled, from male Sprague-Dawley donors) were purchased from Merck KGaA (Darmstadt, Germany), while human hepatic S9 fractions (pooled, from three male donors) were bought from Biopredic International (Saint-Grégoire, France). Specifications of the S9 fractions are provided in Text S1. The reagents of the nicotinamide adenine dinucleotide phosphate (NADPH) regenerating system, namely glucose-6-phosphate dehydrogenase (G6P-DH) from *S. cerevisiae* and glucose-6-phosphate (G6P) disodium salt hydrate (≥98% purity) were purchased from Merck KGaA, while the nicotinamide adenine dinucleotide phosphate disodium salt ($NADP^+$) (≥98% purity) was obtained from Carl Roth GmbH (Karlsruhe, Germany). Components of the incubation phosphate buffer medium, namely dipotassium phosphate (K_2HPO_4) (≥99% purity), magnesium chloride hexahydrate ($MgCl_2$•$6H_2O$) (≥99.5% purity) and disodium ethylenediamine-tetraacetate dihydrate (Na_2EDTA•$2H_2O$) (≥99% purity) were purchased from Carl Roth GmbH (Karlsruhe, Germany).

2.2. In vitro incubation

A series of test assays with different initial surfactant (CF_3-O-SURF, CF_3-S-SURF) concentrations (1, 2, 5, 10, 20, 50, 100, 200 μmol/L (μM)) were performed. Test assays were prepared by adding 1 mg/mL of RL-S9 or HL-S9 and 2.5 μL (1 v/v%) of the corresponding CF_3-O-SURF/CF_3-S-SURF dosing solution (final concentration 1–200 mM, prepared in DMSO) to phosphate buffer (pH = 7.4, 50 mM K_2HPO_4, 3 mM

Table 1
General information about the targeted chemicals of this study. Adapted from Licul-Kucera et al. (2023).

Name	Abbreviation	Structure	Formula	Molecular weight ($gmol^{-1}$)
Parent substances				
1,5-dioxo-1,5-bis({2-[1,1,2-trifluoro-2-(trifluoromethoxy)ethoxy]ethoxy})-3-({2-[1,1,2-trifluoro-2-(trifluoromethoxy)ethoxy]ethoxy}carbonyl) pentane-2-sulfonic acid	CF_3–*O*-SURF	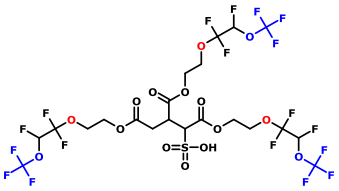	$C_{21}H_{20}F_{18}O_{15}S$	886.41
1,5-dioxo-1,5-bis(2-{[1,1,2-trifluoro-2-(trifluoromethoxy)ethyl]sulfanyl} ethoxy)-3-[(2-{[1,1,2-trifluoro-2-(trifluoromethoxy)ethyl]sulfanyl} ethoxy)carbonyl]pentane-2-sulfonic acid	CF_3–S-SURF	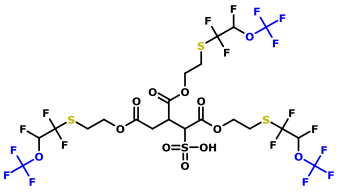	$C_{21}H_{20}F_{18}O_{12}S_4$	934.61
Possible metabolites				
2-[1,1,2-trifluoro-2-(trifluoromethoxy)ethoxy]ethan-1-ol	CF_3–*O*-ALC	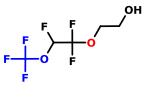	$C_5H_6F_6O_3$	228.09
2-{[1,1,2-trifluoro-2-(trifluoromethoxy)ethyl]sulfanyl}ethan-1-ol	CF_3–S-ALC	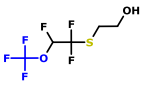	$C_5H_6F_6O_2S$	244.16
[1,1,2-trifluoro-2-(trifluoromethoxy)ethoxy]acetic acid	CF_3–*O*-CA	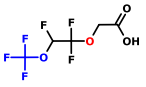	$C_5H_4F_6O_4$	242.07
{[1,1,2-trifluoro-2-(trifluoromethoxy)ethyl]sulfanyl}acetic acid	CF_3–S-CA	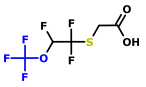	$C_5H_4F_6O_3S$	258.14
Fluoro(trifluoromethoxy)acetic acid	CF_3-CA		$C_3H_2F_4O_3$	162.04

$MgCl_2$•$6H_2O$, 1.2 mM Na_2EDTA•$2H_2O$). They were then pre-incubated for 5 min at 37 °C, with constant shaking. After that NADPH regenerating system (final concentration: 1.0 mM $NADP^+$, 5.0 mM G6P and 2 units/mL G6P-DH) was added to make a final volume of 250 μL. Samples were then incubated at 37 °C, with constant shaking, for 120 min (detailed preliminary optimization of incubation parameters in Text S2 and Fig. S1). Finally, 250 μL of ice-cold MeOH was added to quench the reaction.

2.3. Sample preparation and clean-up

Following incubation, samples were vortexed for 10 s and centrifuged at 4000 rpm for 10 min. The supernatant was collected and then filtered through a 0.2 μm filter. An aliquot of the sample (depending on the initial concentration of parent substance) was then transferred to an autosampler vial and completed to 200 μL volume with 50/50 v/v% MeOH/H_2O and 10 μL of the mix of IS to have a final concentration of 7, 2.5, 1, 1 and 1 μg/L for PFPrA, PFPrS, PFHxA, PFNA or PFDA in the injected sample, respectively.

2.4. Quality assurance and quality control

Applicability and reliability of the incubation method was tested with different control assays run in parallel to each sample batch. Activity of the liver enzymes was checked by the positive control assay, where the test compounds were replaced by metoprolol, a substance, whose metabolism is well-documented in the literature. Reagent blank assay was prepared by adding pure solvent (DMSO) instead of the dosing solution, to determine any background contamination. Heat-inactivated negative control assay was prepared identically to the test assays, but prior to the addition of NADPH regenerating system, it was incubated at 80 °C for 15 min. In this way, enzymes were heat-inactivated, and this control sample enabled the determination of non-enzymatic hydrolysis. In the cofactor-free control assay the test compounds were incubated in the presence of S9 enzymes, but in the absence of the NADPH cofactor. Test assays were prepared in triplicates, while heat-inactivated negative control and cofactor-free control assays were prepared in unicates at different concentration levels. One positive control and reagent blank was prepared for each separate batch of samples.

The MS spectra of the injected positive control assays showed the characteristic peaks of metoprolol metabolites (Fig. S2). The activity of enzymes was therefore justified. No parent compounds or metabolites were found in the reagent blank assays; therefore, no blank correction was needed.

2.5. Instrumental analysis

Quantification was based on a calibration plot which included the parent compounds as well as those transformation products (TPs) for which reference standards were available. Targeted analysis was performed by liquid chromatography–tandem mass spectrometry (LC-MS/MS). For quantification, the internal standard calibration approach was used. As for the target analytes the corresponding mass-labelled chemical was not available, the non-mass labelled PFCA or PFSA which was the closest eluting to the corresponding target substance – namely PFPrA, PFPrS, PFHxA, PFNA or PFDA– was used as IS. Further details are provided in Table S3. Method performance was assessed with the calibration range, instrumental and method limit of detection (LOD) and limit of quantification (LOQ), and recovery described in Text S4. Results are presented in Table S4.

Additional TPs for which reference standards were not available, were identified using an established non-targeted screening workflow on the high-resolution mass spectrometer (HRMS) software. More details on non-targeted screening are provided in the SI section (Text S5 and S6).

2.6. Kinetic modelling

By using OriginPro 2018 software (version SR1-b9.5.1.195, OriginLab Corporation, Northampton, MA, USA), metabolite formation rate against the surfactant (CF_3-O-SURF, CF_3-S-SURF) concentration was plotted and different enzymatic kinetic models were fitted, namely the Michaelis-Menten equation, the Hill equation, and the substrate-inhibition equation (Lipscomb and Poet, 2008). As multiple simultaneous reactions can play a role in the depletion of the parent substance, monitoring the formation of single metabolites separately can be advantageous for the understanding of metabolic pathway. A similar approach was followed in previous studies (Abdallah et al., 2019; Gonsalves et al., 2021; Obringer et al., 2021).

The model which best described all cases was the Michaelis-Menten equation (Equation (1)) (Lipscomb and Poet, 2008).

$$v = \frac{Vmax \times [S]}{K_m + [S]} \quad (1)$$

In the case of the Michaelis-Menten model, the apparent intrinsic *in vitro* clearance (CL_{int}) based on the formation of a certain metabolite can be calculated according to Equation (2) (Lipscomb and Poet, 2008).

$$CL_{int} = \frac{v}{[S]} = \frac{V_{max}}{K_m} \quad (2)$$

As in this study CL_{int} only expresses the metabolic capacity of 1 mg of S9 fraction in the liver, it is more informative to scale up by the protein density of the liver and express the metabolic capacity of 1 g of liver tissue (based on the corresponding subcellular fraction). This intrinsic *in vitro* hepatic clearance ($CL_{int,\ liver}$) on grams of liver basis, can be determined according to Equation (3) (Nishimuta et al., 2014).

$$CL_{int,liver} = CL_{int} \times p \quad (3)$$

In the abovementioned equations v is the initial velocity of the reaction, V_{max} is the maximum rate of enzymatic reaction which is possible for that specific chemical-enzyme interaction, [S] is the surfactant (CF_3-O-SURF, CF_3-S-SURF) concentration, K_m is the Michaelis-Menten constant, and p is the amount of protein per gram of the liver.

After fitting the Michaelis-Menten model, the parameters of the nonlinear function –V_{max} and K_m – were automatically calculated by the software. V_{max} is the rate of the reaction at which the enzyme shows the highest turnover, while K_m is the concentration required to achieve 50% of this maximum reaction rate. For calculation of $CL_{int,\ liver}$, the following parameters were applied: 121 mg protein•g $liver^{-1}$ for HL-S9 (Nishimuta et al., 2014), and 136 mg protein•g $liver^{-1}$ for RL-S9 (Zhou et al., 2020).

3. Results and discussion

3.1. Metabolic pathways

Possible metabolic pathways were predicted by using fundamental knowledge of phase I enzymatic reactions (Lentz et al., 2013) and based on previous findings from microbial biotransformation of the same chemicals (Licul-Kucera et al., 2023). The prototype chemicals are trifunctional esters with aconitic acid – a naturally occurring, tricarboxylic acid – base, which is esterified by adding alcohols made of a trifluoromethoxy group linked to a fluorinated (thio)ethylene glycol derivative. On this basis, initial de-esterification of the surfactants catalyzed by esterase enzymes to release the alcohol, followed by oxidation of the free alcohol to a carboxylic acid by cytochrome P450 (CYP) enzymes via the formation of an aldehyde intermediate was hypothesized. As these carboxylic acids possess a -CHF-CF_2-O/S-CH_2- moiety in the molecule, there is a potential for the consecutive elimination of two HF molecules, initially producing CF_3-CA and then labile trifluoromethanol which further decomposes to HF and CO_2 at ambient

temperature (Zachariah et al., 1995). The proposed transformation pathway is presented on Fig. S3.

3.2. Metabolic profile by targeted analysis

3.2.1. CF_3-O-SURF

In the case of CF_3-O-SURF, no abiotic hydrolysis was observed neither in the heat-inactivated control nor in the cofactor-free control assays. This is in accordance with our previous finding (Licul-Kucera et al., 2023), that the abiotic hydrolysis of the surfactants was only experienced under highly basic conditions (pH = 9) but not in nearly neutral medium such as the phosphate buffer (pH = 7.4).

When incubating with RL-S9, as expected two metabolites, CF_3-O-ALC and CF_3-O-CA were produced. CF_3-O-ALC was detected in similar amounts in the cofactor-free control assay indicating that the biotic hydrolysis is not CYP-induced. Similar results were observed in a study where esters of *p*-hydroxybenzoic acid were incubated with HL-S9 without addition of NADPH regenerating system, yet esterase hydrolysis still occurred (Obringer et al., 2021). Oxidation of CF_3-O-ALC to CF_3-O-CA was most likely induced by CYP enzymes, confirmed by the observation that CF_3-O-CA was formed in test assays but not in the cofactor-free control assays. It is based on the functioning mechanism of CYP enzymes as – in contrast to esterases – they require a reducing agent (usually reduced nicotinamide adenine dinucleotide phosphate, NADPH) (Parkinson et al., 2015).

In the case of incubation with HL-S9, only one metabolite, the oxidation product CF_3-O-CA was formed in low concentrations. Possible explanations to this are that the CF_3-O-ALC was produced in an amount

Table 2
Metabolites of CF_3–*O*-SURF and CF_3–S-SURF identified by HRMS.

Name	Observed in samples incubated with S9 from H/R/H + R[a]	Formula	Proposed structure	*m/z* theoretical	Mass error (ppm)	Retention time (min)	*Confirmation level (Schymanski* et al., *2014)*
CF_3–*O*-SURF							
TP-NTS-O1	R	$C_{12}H_{14}F_6O_{11}S$	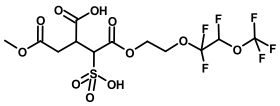	479.0089	0.2	5.18	2b
TP-NTS-O2	R	$C_{14}H_{14}F_6O_9$	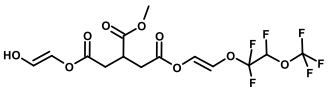	439.0469	0.2	6.96	3
CF_3–S-SURF							
TP-NTS-S1	H	$C_{21}H_{20}F_{18}O_{14}S_4$	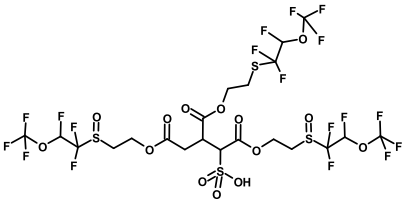	964.9376	1.0	9.39	3
TP-NTS-S2	H + R	$C_{21}H_{20}F_{18}O_{13}S_4$	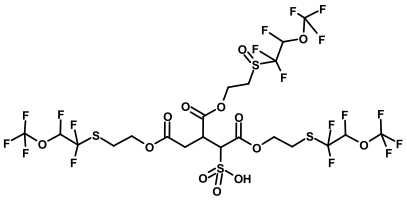	948.9427	−5.3	9.89	2b
TP-NTS-S3	R	$C_{18}H_{20}F_{12}O_{11}S_3$	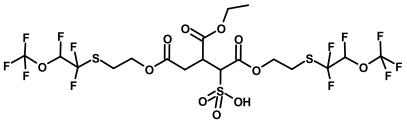	734.9903	0.3	9.40	3
TP-NTS-S4	H + R	$C_{16}H_{16}F_{12}O_{12}S_3$	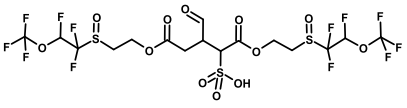	722.9539	1.4	7.56	3
TP-NTS-S5	H + R	$C_5H_6F_6O_3S$	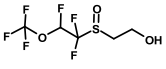	258.9869	−3.9	6.22	2b

[a] Abbreviations:H = human, R = rat, H + R = both human and rat.

<LOD or that the oxidative transformation by CYP occurred more quickly in HL-S9 than in RL-S9. Less plausible is that the transformation of CF_3.O-SURF to CF_3.O-CA in human fractions followed a different pathway than in rat S9 and that CF_3.O-ALC is not an intermediate step in the oxidation. Roberts et al. (2012) also found some species-specific differences in the kinetics of the brominated diester bis(2-ethylhexyl) 2,3,4,5 tetrabromophthalate (TBPH). After the incubation with human liver microsomes, no loss of TBPH or production of hydrolysis metabolite was observed. However, it was slowly metabolized in the presence of porcine hepatic carboxylesterase (Roberts et al., 2012).

3.2.2. CF_3.S-SURF

The metabolic profile of CF_3.S-SURF was similar to that of CF_3.O-SURF. First, no abiotic hydrolysis was observed neither in the heat-inactivated control assays nor in the cofactor-free control assays. During the incubation with RL-S9, both CF_3.S-ALC and CF_3.S-CA were detected. CF_3.S-ALC was also present in the cofactor-free control assays when using RL-S9. The sole metabolite formed with HL-S9 was CF_3.S-CA. This difference in the metabolic profile with the enzymes from two distinct species may be explained in similar fashion to CF_3.O-SURF.

3.3. Metabolic profile by non-targeted analysis

Following the post-acquisition data filtration steps (described in Text S6), two additional metabolites with unequivocal molecular formula and possible structure (at least level 3 identification confidence, according to Schymanski et al., 2014) of CF_3.O-SURF was found (Table 2). The structures were confirmed by using the spectral information, e.g., production of acetate adducts, isotope patterns and diagnostic MS/MS fragments produced in MS/MS.

TP-NTS-O1 was an intermediate likely produced from CF_3.O-SURF by cleaving two moieties of the fluorinated wings of the molecule. TP-NTS-O2 was originated from TP-NTS-O1 by cleaving the sulfonate group.

However, for CF_3.S-SURF, five additional transformation products with a minimum of level 3 identification confidence were identified (Table 2). TP-NTS-S1 was a di-oxidized molecule where the two oxygen atoms were either both linked to one of the thioether groups or to two different ones. The relative position of the two oxygens could not be determined in our experiments (level 3). TP-NTS-S2 was a mono-oxidized molecule where the single oxygen atom was linked to one of the equivalent thioether groups. Based on the diagnostic fragments, the isotope pattern and the experimental context, the structure could unambiguously be assigned (level 2b). The third metabolite (TP-NTS-S3) was likely produced from the CF_3.S-SURF by cleaving a moiety of the fluorinated wing of the molecule. TP-NTS-S4 was probably formed from TP-NTS-S1 by cleaving a moiety of the fluorinated wings of the molecule. Like in TP-NTS-S1, the relative position of the two oxygens could not be unequivocally determined (level 3). The smallest metabolite (TP-NTS-S5) identified by HRMS was the oxidized CF_3.S-ALC, where the oxygen atom was linked to the thioether group. This structure was confirmed based on the presence of the MS/MS fragment $CHOS^-$ which unequivocally determined the position of the oxygen. Moreover, this molecule was also detected in the form of an acetate adduct which is a typical phenomenon reported for fluorinated alcohols (Berger et al., 2004). In RL-S9 incubations, TP-NTS-S1 was not present, while in samples incubated with HL-S9, TP-NTS-S3 was not detected. These metabolites – except TP-NTS-S2 – were detected with very low intensities. Table 2 summarizes the information of the findings of the non-targeted analysis.

3.4. Metabolism kinetics

As the decrease in the concentration of the parent substances in the given test time was too small to be monitored over time, and based on the original approach of the Michaelis-Menten equation (Atkins, 2005; Tomczak and Weglarz-Tomczak, 2019), the formation of metabolites analyzed by targeted analysis was monitored rather than the loss of surfactants (CF_3.O-SURF, CF_3.S-SURF). The production of metabolites was plotted against the dosing concentration of the parent compound. The estimated kinetic parameters for formation of the metabolites as well as the calculated *in vitro* hepatic clearance values are presented in Table 3. Comparable calculations were not performed for the metabolites analyzed by non-targeted analysis as these could not be quantified because of lack of standards.

3.4.1. CF_3.O-SURF

The plotted results showed formation of metabolite CF_3.O-CA was best fitted by the Michaelis-Menten model both in the HL-and RL-S9 incubation (Fig. 1B). However, CF_3.O-ALC – which was only formed in the RL-S9 assays – did not fit any of the possible enzyme kinetic models (Fig. 1A). In fact, it did not reach saturation in the observed concentration range, indicating that steady state was not achieved. The lack of steady state condition for CF_3.O-ALC precluded the determination of its kinetic parameters using kinetic models.

The predicted maximum metabolic rates (V_{max}) for production of the metabolite CF_3.O-CA were 512 (±20) and 3974 (±192) fmol min^{-1} mg $protein^{-1}$ in HL-S9 and RL-S9 assays, respectively (Table 3). K_m values were 136 (±10) and 66 (±8) μM for HL-S9 and RL-S9, respectively (Table 3). The corresponding CL_{int} and $CL_{int,\ liver}$ values calculated according to Eqs. (2) and (3) are reported in Table 3.

3.4.2. CF_3.S-SURF

For CF_3.S-SURF, formation of both CF_3.S-ALC and CF_3.S-CA metabolites was best fitted to the Michaelis-Menten model (Fig. 1C and D). However, as stated above, CF_3.S-ALC was only formed during reaction with RL-S9. The V_{max} value for production of metabolite CF_3.S-ALC in RL-S9 was 704 200 (±19 633) fmol min^{-1} mg $protein^{-1}$. For CF_3.S-CA, the calculated V_{max} were 5016 (±842) and 4675 (±90) fmol min^{-1} mg $protein^{-1}$ in the HL-S9 and RL-S9 assays, respectively (Table 3). K_m values were 178 (±52) and 29 (±2) μM for HL-S9 and RL-S9, respectively (Table 3). The corresponding CL_{int} and $CL_{int,\ liver}$ values calculated based on Eqs. (2) and (3) are presented in Table 3.

3.5. Inter-species and -congeners metabolic comparison

The metabolic profile of CF_3.O-SURF and CF_3.S-SURF observed with the human and rat *in vitro* S9 assays only differed in terms of the formation of the corresponding alcohol CF_3.O-ALC or CF_3.S-ALC only following the RL-S9 incubation. This, however, might be linked to the deviation in the rate of the hydrolysis reaction as described under section 3.2.1 above. Nabb et al. also found difference in the type of metabolites formed when an isotopically labelled PFAS, 8:2 fluorotelomer alcohol (8:2 FTOH) was incubated with rat, mouse, and human liver microsomes and cytosol (Nabb et al., 2007). The production of species-specific metabolites was reported in one study for other halogenated substances. For instance, the various diastereomers of the brominated flame retardant, hexabromocyclododecane (HBCDD) produced metabolites which were exclusively detected either with rat or trout S9 fractions (Abdallah et al., 2014). A metabolic product of another flame retardant, TBPH, was exclusively formed *in vitro* by porcine enzymes, but not in human or rat subcellular fractions (Roberts et al., 2012). When incubating a short-chained chlorinated paraffin, 1, 2, 5, 5, 6, 9, 10-heptachlorodecane (HeptaCD) with chicken and human microsomes, two metabolites were detected in human liver microsomal assays, while only one metabolite was identified in chicken liver microsomal assays (Lin et al., 2022).

The conspicuous species differences in our study were revealed by comparing the metabolic rate obtained using HL-S9 with that observed when using RL-S9 enzymes. The most prominent difference in the metabolic rate of the two surfactants was delivered by the formation of the primary metabolites CF_3.O-ALC and CF_3.S-ALC. The formation rate

Table 3
Kinetic parameters derived from Michaelis-Menten model for the formation of CF_3–*O*-CA and CF_3–S-CA following incubation with RL- and HL-S9. The ± values represent standard error values.

Metabolite	Species	V_{max} ($fmol \bullet min^{-1} \bullet mg^{-1}$)	K_m (μM)	CL_{int} ($nL \bullet min^{-1} \bullet mg^{-1}$)	$CL_{int,\ liver}$ ($\mu L \bullet min^{-1} \bullet g\ liver^{-1}$)
CF_3–O-ALC	Human	–	–	–	–
	Rat	–	–	–	–
CF_3–S-ALC	Human	–	–	–	–
	Rat	704 200 ± 19 633	130 ± 9	5402 ± 2288	735 ± 311
CF_3–O-CA	Human	512 ± 20	136 ± 10	4 ± 2	0.45 ± 0.24
	Rat	3973 ± 192	66 ± 8	61 ± 25	8.23 ± 3.39
CF_3–S-CA	Human	5016 ± 842	178 ± 52	28 ± 16	3.41 ± 1.96
	Rat	4675 ± 90	29 ± 2	162 ± 52	22.0 ± 7.1

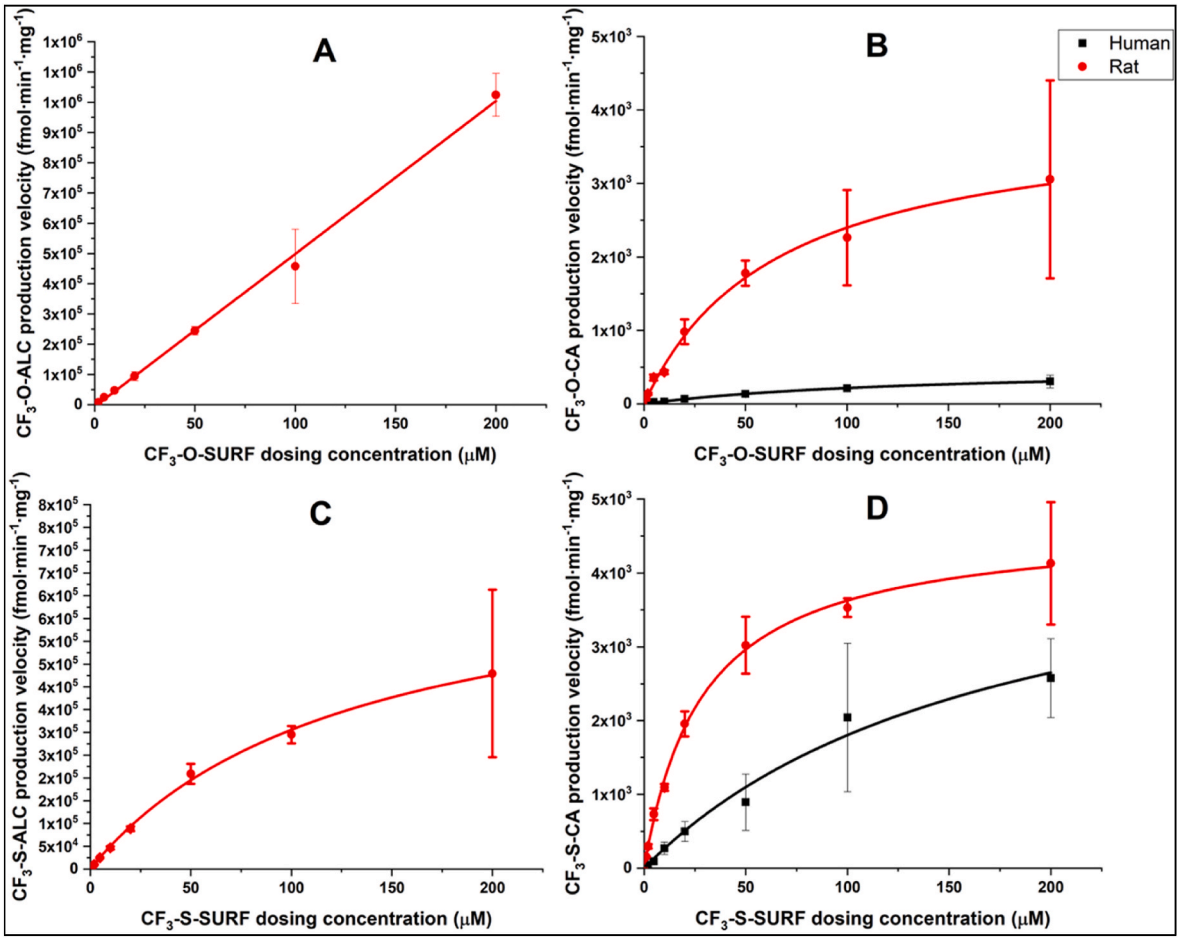

Fig. 1. Kinetics of A) CF_3.O-ALC, B) CF_3.O-CA, C) CF_3.S-ALC and D) CF_3.S-CA production during incubation with rat and human S9 hepatic fractions, using the Michaelis-Menten model. Error bars represent standard deviations. (n = 3).

of primary metabolite CF_3.S-ALC (704 200 ± 19 633 fmol $min^{-1} \cdot min^{-1}$) was 150-times higher than that of the secondary metabolite CF_3.S-CA (4675 ± 90 fmol $min^{-1} \cdot min^{-1}$) in rat. Even though an explicit V_{max} value of the CF_3.O-ALC cannot be determined (no steady-state condition), its V_{max} should also exceed by at least two orders of magnitudes that of CF_3.O-CA. This indicates that the overall metabolic rate and clearance of both CF_3.O-SURF and CF_3.S-SURF is significantly higher in rat liver than in human liver. Therefore, it can be concluded that the use of animal models in metabolic and toxicity tests as indicators of human hazard can lead to serious mispredictions in some cases.

The V_{max} values indicate that formation rate of CF_3.O-CA was about 8-times higher in rats (3973 ± 192 fmol $min^{-1} \cdot min^{-1}$) than in humans (512 ± 20 fmol $min^{-1} \cdot min^{-1}$), while that of CF_3.S-CA was similar in the two species (5016 ± 842 and 4675 ± 90 fmol $min^{-1} \cdot min^{-1}$). The CL_{int} values revealed about 18 (8234 ± 3386 vs 454 ± 239 nL $min^{-1} \bullet g^{-1}$ liver) and 6.5-times (22 026 ± 7094 vs 3405 ± 1960 nL $min^{-1} \bullet g^{-1}$ liver) higher clearance in rat liver than in human liver, for CF_3.O-CA and CF_3.S-CA, respectively. The lower K_m values in rats (66 ± 8 μM and 29 ± 2 μM) compared to humans (136 ± 10 μM and 178 ± 52 μM) for both CF_3.O-CA and CF_3.S-CA suggest higher enzyme specificity in rat (Table 3, Fig. 1). In a previous study, metabolism of 2-ethylhexyl-2,3,4,5-tetrabromobenzoate (TBB) occurred significantly faster in the presence of RLM than with HLM; however, it was similar to the rate seen with porcine liver enzymes (Roberts et al., 2012). For HBCDD diastereomers, the metabolic rate was much slower in trout than rat (Abdallah et al., 2014); while for HeptaCD it was faster for human than for chicken liver microsomes (Lin et al., 2022).

In the current study, the two studied surfactants (CF_3.O-SURF, CF_3.S-SURF) are congeners (i.e., chemical substances related to each other by structure). The maximum formation rate of CF_3.S-CA was 10-times

higher than of CF_3-O-CA (5016 ± 842 vs 512 ± 20 fmol min^{-1}·min^{-1}) in human, while they were similar (3972 ± 192 and 4675 ± 90 fmol min^{-1}·min^{-1}) in rat. When comparing the CL_{int} values of the two congeners, CF_3-S-CA clearance was 7.5-times (3405 ± 1960 vs 454 ± 239 nL min^{-1}•g^{-1} liver) and 2.7-times (22 026 ± 7094 vs 8234 ± 3386 nL min^{-1}•g^{-1} liver) higher than clearance of CF_3-O-CA by HL-S9 and RL-S9, respectively (Table 3, Fig. 1B and D). Abdallah et al. (2014) also reported different metabolic rates of three HBCDD diastereomers during phase I metabolism. Whereas β-HBCDD underwent rapid biotransformation, α-HBCDD was the most resistant to metabolic degradation in both rat and trout (Abdallah et al., 2014). In another hepatic *in vitro* metabolic study, TBB was easily metabolized even without the addition of any cofactor, while no metabolites were detected for TBPH in human or rat subcellular fractions, only by porcine carboxylesterase (Roberts et al., 2012).

3.6. Comparison to other PFAS and implications for exposure

The V_{max} and $CL_{int,\ liver}$ values of the novel prototype PFAS addressed in this study were found to be several orders of magnitude smaller than those for PFAS reported elsewhere (Table 4). The transformation rate of metabolite CF_3-O-CA by HL-S9 was about 2 × 10^3-times and 4 × 10^2-times lower than the degradation rate of 6:2 FTOH and 8:2 FTOH with HLM (Daramola and Rand, 2021; Li et al., 2009; Nabb et al., 2007). Moreover, the transformation rate of metabolite CF_3-S-CA by HL-S9 was about 2 × 10^2-times and 4 × 10^1-times lower than the degradation rate of 6:2 FTOH and 8:2 FTOH when incubating with HLM, respectively (Daramola and Rand, 2021; Nabb et al., 2007). It was also concluded that CF_3-O-CA (3.97 pmol min^{-1}•mg^{-1}) and CF_3-S-CA (5.02 pmol min^{-1}•mg^{-1}) was formed with a similar rate as PFOA from 8:2 FTOH in rat liver (Table 4). The depletion rate of 6:2 and 8:2 FTOH (945 and 204 pmol min^{-1}•mg^{-1}) by HLM was more effective than the formation rate of CF_3-O-ALC or CF_3-S-ALC by HL-S9 – which were negligible. While the V_{max} of CF_3-S-ALC (704 pmol min^{-1}•mg^{-1}) by RL-S9 was in the same order of magnitude as the depletion rate of 6:2 FTOH (945 pmol min^{-1}•mg^{-1}) and 8:2 FTOH (204 pmol min^{-1}•mg^{-1}) by HLM and that of 8:2 fluorotelomer acrylate (8:2 FTAc) (415 pmol min^{-1}•mg^{-1}) by rainbow trout microsomes (Table 4). A summary of V_{max}, K_m and $CL_{int,\ liver}$ values of the novel prototype PFAS and several other PFAS is presented in Table 4.

Overall, these results suggest that metabolism of CF_3-O-SURF and CF_3-S-SURF followed a similar trend to that of 6:2 FTOH or 8:2 FTOH (Daramola and Rand, 2021; Li et al., 2016; Nabb et al., 2007). Namely, metabolism was significantly slower in humans, but faster in rats. The depletion of parent substances/formation of primary metabolites as well as the formation of dead-end metabolites (e.g., CF_3-O-CA, CF_3-S-CA, PFOA) were of the same order of magnitude in rat liver (Table 4).

It has been shown in previous studies that the metabolism of the PFAS precursors FTOHs lead to the production of more toxic, e.g., fluorotelomer aldehyde, and/or highly persistent and bioaccumulative (PFAAs) metabolites (Butt et al., 2010; Li et al., 2016; Martin et al., 2005; Nabb et al., 2007). On the contrary, these prototype chemicals metabolize to short-chained products which have a similar structure to metabolites investigated by Folkerson et al. and have been found non-bioaccumulative (Folkerson et al., 2021). Further knowledge about the bioaccumulation, mobility and toxicity of the parent substances and their metabolites, is crucial to come to risk assessment for the tested prototype surfactants CF_3-O-SURF and CF_3-S-SURF.

3.7. Study limitations

In vitro assays are low-cost models for predicting the metabolic activity of a xenobiotic. Despite the extensive use of this methodology in the pharmaceutical industry, it has been reported that *in vivo* clearance calculated based on *in vitro* clearance values is often over-or under-predicted when compared to empirical studies (Wood et al., 2017). For example, when Folkerson et al. investigated both *in vitro* and *in vivo* metabolism of a prototype surfactant in rat, the *in vitro* experiment

Table 4
Comparison of the intrinsic in vitro hepatic clearance values of PFAS.

Monitoring substrate depletion or metabolite formation	Substrate	Metabolite monitored	Species	Subcellular fraction	V_{max} (pmol•min^{-1}•mg^{-1})	K_m (μM)	$CL_{int,\ liver}$ (μL•min^{-1}•g $liver^{-1}$)	Reference
Formation	CF_3–*O*-SURF	CF_3–*O*-CA	Human	S9	0.512	136	0.453	This study
Formation	CF_3–*O*-SURF	CF_3–*O*-CA	Rat	S9	3.97	65.6	8.23	This study
Formation	CF_3–S-SURF	CF_3–S-CA	Human	S9	5.02	178	3.41	This study
Formation	CF_3–S-SURF	CF_3–S-CA	Rat	S9	4.68	28.9	22.0	This study
Formation	CF_3–S-SURF	CF_3–S-ALC	Rat	S9	704	130	735	This study
Depletion[a]	6:2 FTOH	–	Human	microsomes	945	11.2	48720	Daramola and Rand, 2021
Depletion[a]	8:2 FTOH	–	Human	microsomes	204	18.5	640	Li et al., 2016
Depletion[b]	8:2 FTOH	–	Rat	microsomes	no data	no data	1832	Nabb et al., 2007
Formation	8:2 FTOH	PFOA	Rat	microsomes	4.1	no data	no data	Nabb et al., 2007
Depletion	8:2 FTOH	–	Human	microsomes	no data	no data	not measurable	Nabb et al., 2007
Formation	8:2 FTOH	PFOA	Human	microsomes	not detected	no data	not detected	Nabb et al., 2007
Depletion[a]	8:2 FTAc	–	Rainbow trout	S9	415	0.342	184 444	Butt et al., 2010

Standard error or deviation was not presented as not all of the presented studies reported it.

[a] The study solely reported CL_{int} value. Hereby $CL_{int,\ liver}$ was calculated using Eq. 3, assessing the protein mg/gram of liver tissue (p) being 58 and 152 mg g $liver^{-1}$. for rat liver microsomes and rainbow trout S9.

[b] Only the $CL_{int,\ liver}$ value normalized to bodyweight was reported. Hereby $CL_{int,\ liver}$ was calculated using the following equation, where w is the weight of liver (g) per kilogram bodyweight, being 12.5 g/0.25 kg for rat according to (Nabb et al., 2007). $CL_{int,liver,bw} = \frac{CL_{int,liver,bw}}{w}$

underestimated the metabolic rate *in vivo* (Folkerson et al., 2021). These results suggest the need for *in vivo* studies to realistically determine the half-life of xenobiotics. However, in terms of the identification of produced metabolites, the *in vitro* assay provided an adequate representation of the *in vivo* system (Folkerson et al., 2021).

It is important to highlight some factors which can influence the results of this study. Namely, physicochemical property data, including water solubility and critical micelle concentration (CMC), were unfortunately not available. However, some *in silico*-based prediction methods were used to predict the water solubility and acid dissociation constant (p*K*a) and of the surfactants. Big discrepancies between the different solubility models were found (Table S2). The calculated p*K*a values, however, clearly suggested that both surfactants were in ionic form at pH = 7.4. Moreover, the co-solvent DMSO was also used to enhance their solubility. Therefore, we assume that the solubility of the test chemicals could not cause any artifacts, not even at the highest concentrations. However, in the absence of any theoretical or experimental data on CMC, the formation of non-bioavailable micelles in the reaction medium cannot be ruled out. Another limitation of this study is that only phase I metabolism was investigated. However, as shown in previous studies, fluorinated substances often also produce phase II conjugates in relevant amounts. In the case of FTOHs, glucuronide, sulfate, glutathione and taurine conjugates were identified during *in vitro* incubations (Li et al., 2016; Martin et al., 2005; Nabb et al., 2007). According to Martin et al. and Li et al., phase II conjugation is the major transformation and excretion route of 8:2 FTOH (Li et al., 2016; Martin et al., 2005). In an *in vivo* experiment, rats were dosed with polyfluoroalkyl phosphate esters. After its hydrolysis to FTOH, glucuronide conjugates were observed at 2 h and 6 h postdosing, and sulfate conjugates were detected between 6 h and 2 days postdosing (D'eon and Mabury, 2011). Also, even though the S9 fraction used in this study are pools from more than one individual, intra-species variations (e.g., sex, age) could not be accounted for.

Therefore, further studies investigating phase II metabolism, as well as *in vivo* experiments are required for comprehensive understanding of metabolic pathways and kinetics, and to be able to assess the health effects of these compounds. Overall, the present study enhances understanding the fate and behavior of these novel prototype fluorinated compounds in different types of organisms. Through characterization of formed metabolites and comparison of transformation rates across species, our results may serve as a basis for future risk evaluation.

CRediT authorship contribution statement

Viktória Licul-Kucera: Conceptualization, Data curation, Formal analysis, Investigation, Methodology, Visualization, Writing – original draft. **Oddný Ragnarsdóttir:** Conceptualization, Data curation, Formal analysis, Investigation, Methodology, Writing – original draft. **Tobias Frömel:** Methodology, Supervision. **Annemarie P. van Wezel:** Funding acquisition, Resources, Supervision, Writing – review & editing. **Thomas P. Knepper:** Funding acquisition, Resources, Writing – review & editing. **Stuart Harrad:** Funding acquisition, Resources, Supervision, Writing – review & editing. **Mohamed Abou-Elwafa Abdallah:** Conceptualization, Methodology, Supervision, Writing – review & editing.

Declaration of competing interest

The authors declare that they have no known competing financial interests or personal relationships that could have appeared to influence the work reported in this paper.

Data availability

Data will be made available on request.

Acknowledgement

The authors acknowledge the funding from the European Union's Horizon 2020 research and innovation programme under the Marie Skłodowska-Curie grant agreement No 860665. Reiner Friedrich and Merck KGaA (Darmstadt, Germany) are acknowledged for the design and synthesis of the test chemicals addressed in this study, as well as the discussion throughout the work. The IUPAC names of the prototype surfactants were generated by MarvinSketch (version 23.5.0, ChemAxon Ltd., Budapest, Hungary) which was available for us for free. Eszter Borsos (University of Vienna) is thanked for her advice and guidance in performing and evaluating the metabolism experiments.

Appendix A. Supplementary data

Supplementary data to this article can be found online at https://doi.org/10.1016/j.chemosphere.2024.141237.

References

Abdallah, M.A.E., Uchea, C., Chipman, J.K., Harrad, S., 2014. Enantioselective biotransformation of hexabromocyclododecane by in vitro rat and trout hepatic subcellular fractions. Environ. Sci. Technol. 48, 2732–2740. https://doi.org/10.1021/es404644s.

Abdallah, M.A.E., Nguyen, K.H., Moehring, T., Harrad, S., 2019. First insight into human extrahepatic metabolism of flame retardants: biotransformation of EH-TBB and Firemaster-550 components by human skin subcellular fractions. Chemosphere 227, 1–8. https://doi.org/10.1016/j.chemosphere.2019.04.017.

Atkins, W.M., 2005. Non-Michaelis-Menten kinetics in cytochrome P450-catalyzed reactions. Annu. Rev. Pharmacol. Toxicol. 45, 291–310. https://doi.org/10.1146/annurev.pharmtox.45.120403.100004.

Berger, U., Langlois, I., Oehme, M., Kallenborn, R., 2004. Comparison of three types of mass spectrometer for high-performance liquid chromatography/mass spectrometry analysis of perfluoroalkylated substances and fluorotelomer alcohols. Eur. J. Mass Spectrom. 10, 579–588. https://doi.org/10.1255/ejms.679.

Björnsdotter, M.K., Hartz, W.F., Kallenborn, R., Ericson Jogsten, I., Humby, J.D., Kärrman, A., Yeung, L.W.Y., 2021. Levels and seasonal trends of C1–C4 perfluoroalkyl acids and the discovery of trifluoromethane sulfonic acid in surface snow in the arctic. Environ. Sci. Technol. https://doi.org/10.1021/acs.est.1c04776.

Buck, R.C., Franklin, J., Berger, U., Conder, J.M., Cousins, I.T., Voogt, P. De, Jensen, A. A., Kannan, K., Mabury, S.A., van Leeuwen, S.P.J., 2011. Perfluoroalkyl and polyfluoroalkyl substances in the environment: terminology, classification, and origins. Integrated Environ. Assess. Manag. 7, 513–541. https://doi.org/10.1002/ieam.258.

Butt, C.M., Muir, D.C.G., Mabury, S.A., 2010. Biotransformation of the 8:2 fluorotelomer acrylate in rainbow trout. 2. In vitro incubations with liver and stomach S9 fractions. Environ. Toxicol. Chem. 29, 2736–2741. https://doi.org/10.1002/etc.348.

Cao, H., Zhou, Z., Hu, Z., Wei, C., Li, J., Wang, L., Liu, G., Zhang, J., Wang, Y., Wang, T., Liang, Y., 2022. Effect of enterohepatic circulation on the accumulation of per- and poly fl uoroalkyl substances: evidence from experimental and computational studies. Environ. Sci. Technol. 56, 3214–3224. https://doi.org/10.1021/acs.est.1c07176.

Coggan, T.L., Anumol, T., Pyke, J., Shimeta, J., Clarke, B.O., 2019. A single analytical method for the determination of 53 legacy and emerging per- and polyfluoroalkyl substances (PFAS) in aqueous matrices. Anal. Bioanal. Chem. 411, 3507–3520. https://doi.org/10.1007/s00216-019-01829-8.

Cousins, I.T., Johansson, J.H., Salter, M.E., Sha, B., Scheringer, M., 2022. Outside the safe operating space of a new planetary boundary for per- and polyfluoroalkyl substances (PFAS). Environ. Sci. Technol. 56, 11172–11179. https://doi.org/10.1021/acs.est.2c02765.

Daramola, O., Rand, A.A., 2021. Emerging investigator series: human CYP2A6 catalyzes the oxidation of 6:2 fluorotelomer alcohol. Environ. Sci. Process. Impacts 23, 1688–1695. https://doi.org/10.1039/d1em00307k.

DeWitt, J.C., Blossom, S.J., Schaider, L.A., 2019. Exposure to per-fluoroalkyl and polyfluoroalkyl substances leads to immunotoxicity: epidemiological and toxicological evidence. J. Expo. Sci. Environ. Epidemiol. 29, 148–156. https://doi.org/10.1038/s41370-018-0097-y.

D'eon, J.C., Mabury, S.A., 2011. Exploring indirect sources of human exposure to perfluoroalkyl carboxylates (PFCAs): evaluating uptake, elimination, and biotransformation of polyfluoroalkyl phosphate esters (PAPs) in the Rat. Environ. Health Perspect. 119, 344–350. https://doi.org/10.1289/ehp.1002409.

European Chemical Agency, 2019. Inclusion of Substances of Very High Concern in the Candidate List for Eventual Inclusion in Annex XIV. ED/71/2019.

European Chemical Agency, 2022. Inclusion of Substances of Very High Concern in the Candidate List for Eventual Inclusion in Annex XIV Distribution. D(2022)9120-DC Public.

European Chemicals Agency, 2017. Guidance on Information Requirements and Chemical Safety Assessment. Chapter R. 11: PBT/vPvB assessment. https://doi.org/10.2823/128621.

European Commission, 2021. Commission regulation (EU) 2021/1297 of 4 August 2021 amending Annex XVII to Regulation (EC) No 1907/2006 of the European Parliament

and of the Council as regards perfluorocarboxylic acids containing 9 to 14 carbon atoms in the chain (C9-C14 PFCAs), their. Off. J. Eur. Union 282, 29–33.
Fasano, W.J., Carpenter, S.C., Gannon, S.A., Snow, T.A., Stadler, J.C., Kennedy, G.L., Buck, R.C., Korzeniowski, S.H., Hinderliter, P.M., Kemper, R.A., 2006. Absorption, distribution, metabolism, and elimination of 8-2 fluorotelomer alcohol in the rat. Toxicol. Sci. 91, 341–355. https://doi.org/10.1093/toxsci/kfj160.
Folkerson, A.P., Joudan, S., Mabury, S.A., D'eon, J.C., 2021. In vivo transformation of a novel polyfluoroether surfactant. Environ. Toxicol. Chem. 00, 1–9. https://doi.org/10.1002/etc.5230.
Gardener, H., Sun, Q., Grandjean, P., 2021. PFAS concentration during pregnancy in relation to cardiometabolic health and birth outcomes. Environ. Res. 192, 110287 https://doi.org/10.1016/j.envres.2020.110287.
Glüge, J., Scheringer, M., Cousins, I.T., DeWitt, J.C., Goldenman, G., Herzke, D., Lohmann, R., Ng, C.A., Trier, X., Wang, Z., 2020. An overview of the uses of per- and polyfluoroalkyl substances (PFAS). Environ. Sci. Process. Impacts Implic. 22, 2345–2373. https://doi.org/10.1039/d0em00291g.
Gonsalves, M.D., Colizza, K., Smith, J.L., Oxley, J.C., 2021. In vitro and in vivo studies of triacetone triperoxide (TATP) metabolism in humans. Forensic Toxicol. 39, 59–72. https://doi.org/10.1007/s11419-020-00540-z.
González-Barreiro, C., Martínez-Carballo, E., Sitka, A., Scharf, S., Gans, O., 2006. Method optimization for determination of selected perfluorinated alkylated substances in water samples. Anal. Bioanal. Chem. 386, 2123–2132. https://doi.org/10.1007/s00216-006-0902-7.
Grandjean, P., Heilmann, C., Weihe, P., Nielsen, F., Mogensen, U.B., Timmermann, A., Budtz-Jørgensen, E., 2017. Estimated exposures to perfluorinated compounds in infancy predict attenuated vaccine antibody concentrations at age 5-years. J. Immunot. 14, 188–195. https://doi.org/10.1080/1547691X.2017.1360968.
Gremmel, C., Frömel, T., Knepper, T.P., 2017. HPLC–MS/MS methods for the determination of 52 perfluoroalkyl and polyfluoroalkyl substances in aqueous samples. Anal. Bioanal. Chem. 409, 1643–1655. https://doi.org/10.1007/s00216-016-0110-z.
Hale, S.E., Arp, H.P.H., Schliebner, I., Neumann, M., 2020. Persistent, mobile and toxic (PMT) and very persistent and very mobile (vPvM) substances pose an equivalent level of concern to persistent, bioaccumulative and toxic (PBT) and very persistent and very bioaccumulative (vPvB) substances under REACH. Environ. Sci. Eur. 32 https://doi.org/10.1186/s12302-020-00440-4.
Janousek, R.M., Lebertz, S., Knepper, T.P., 2019. Previously unidentified sources of perfluoroalkyl and polyfluoroalkyl substances from building materials and industrial fabrics. Environ. Sci. Process. Impacts 21, 1936–1945. https://doi.org/10.1039/c9em00091g.
Kola, I., Landis, J., 2004. Can the pharmaceutical industry reduce attrition rates? Nat. Rev. Drug Discov. 3, 711–715. https://doi.org/10.1038/nrd1470.
Lau, C., Anitole, K., Hodes, C., Lai, D., Pfahles-Hutchens, A., Seed, J., 2007. Perfluoroalkyl acids: a review of monitoring and toxicological findings. Toxicol. Sci. 99, 366–394. https://doi.org/10.1093/toxsci/kfm128.
Lentz, K., Raybon, J., Sinz, M.W., 2013. Drug metabolism and pharmacokinetics in drug discovery. In: Drug Discovery: Practices, Processes, and Perspectives, pp. 99–139. https://doi.org/10.1002/9781118354483.ch4.
Li, B., Zhang, T., Xu, Z., Fang, H.H.P., 2009. Rapid analysis of 21 antibiotics of multiple classes in municipal wastewater using ultra performance liquid chromatography-tandem mass spectrometry. Anal. Chim. Acta 645, 64–72. https://doi.org/10.1016/j.aca.2009.04.042.
Li, Z.M., Guo, L.H., Ren, X.M., 2016. Biotransformation of 8:2 fluorotelomer alcohol by recombinant human cytochrome P450s, human liver microsomes and human liver cytosol. Environ. Sci. Process. Impacts 18, 538–546. https://doi.org/10.1039/c6em00071a.
Licul-Kucera, V., Frömel, T., Kruså, M., van Wezel, A.P., Knepper, T.P., 2023. Finding a way out? Comprehensive biotransformation study of novel fluorinated surfactants. Chemosphere 339. https://doi.org/10.1016/j.chemosphere.2023.139563.
Lin, L., Abdallah, M.A.E., Chen, L.J., Luo, X.J., Mai, B.X., Harrad, S., 2022. Comparative in vitro metabolism of short chain chlorinated paraffins (SCCPs) by human and chicken liver microsomes: first insight into heptachlorodecanes. Sci. Total Environ. 851, 158261 https://doi.org/10.1016/j.scitotenv.2022.158261.
Lipscomb, J.C., Poet, T.S., 2008. In vitro measurements of metabolism for application in pharmacokinetic modeling. Pharmacol. Ther. 118, 82–103. https://doi.org/10.1016/j.pharmthera.2008.01.006.
Martin, J.W., Mabury, S.A., O'Brien, P.J., 2005. Metabolic products and pathways of fluorotelomer alcohols in isolated rat hepatocytes. Chem. Biol. Interact. 155, 165–180. https://doi.org/10.1016/j.cbi.2005.06.007.
Nabb, D.L., Szostek, B., Himmelstein, M.W., Mawn, M.P., Gargas, M.I., Sweeney, L.M., Stadler, J.C., Buck, R.C., Fasano, W.J., 2007. In vitro metabolism of 8-2 fluorotelomer alcohol: interspecies comparisons and metabolic pathway refinement. Toxicol. Sci. 100, 333–344. https://doi.org/10.1093/toxsci/kfm230.
Nishimuta, H., Houston, J.B., Galetin, A., 2014. Hepatic, intestinal, renal, and plasma hydrolysis of prodrugs in human, cynomolgus monkey, dog, and rat: implications for in vitro-in vivo extrapolation of clearance of prodrugs. Drug Metab. Dispos. 42, 1522–1531. https://doi.org/10.1124/dmd.114.057372.
Federal Institute for, Occupational Safety and Health, National Institute for Public Health and the Environment, Swedish Chemicals Agency, Norwegian Environment Agency, T.D.E.P.A., 2023. Annex XV Restriction Report, Proposal for Restriction, Substance Names(s): Per- and Polyfluoroalkyl Substances (PFASs).
Obringer, C., Wu, S., Troutman, J., Karb, M., Lester, C., 2021. Effect of chain length and branching on the in vitro metabolism of a series of parabens in human liver S9, human skin S9, and human plasma. Regul. Toxicol. Pharmacol. 122, 104918 https://doi.org/10.1016/j.yrtph.2021.104918.
OECD, 2021. Reconciling Terminology of the Universe of Per- and Polyfluoroalkyl Substances: Recommendations and Practical Guidance, Series on Risk Management No.61. (Accessed 18 September 2023).
Osakwe, O., 2016. Preclinical in vitro studies: development and applicability. In: Social Aspects of Drug Discovery, Development and Commercialization. Academic Press, pp. 129–148.
Parkinson, A., Ogilvie, B.W., Buckley, D.B., Kazmi, F., Czerwinski, M., Parkinson, O., 2015. Biotransformation of xenobiotics. In: Klaassen, C.D., Watkins III J B (Eds.), Casarett & Doull's Essentials of Toxicology, 3e. McGraw-Hill Education, New York, NY.
Preston, E.V., Webster, T.F., Henn, B.C., Mcclean, M.D., Oken, E., Rifas-shiman, S.L., Pearce, E.N., Antonia, M., Fleisch, A.F., Sagiv, S.K., 2021. Prenatal exposure to per- and polyfluoroalkyl substances and maternal and neonatal thyroid function in the project viva cohort: a mixtures approach. Environ. Int. 139, 1–26. https://doi.org/10.1016/j.envint.2020.105728.Prenatal.
Roberts, S.C., Macaulay, L.J., Stapleton, H.M., 2012. In vitro metabolism of the brominated flame retardants 2- ethylhexyl-2,3,4,5-tetrabromobenzoate (TBB) and bis(2-ethylhexyl) 2,3,4,5-tetrabromophthalate (TBPH) in human and rat tissues. Chem. Res. Toxicol. 25, 1435–1441. https://doi.org/10.1021/tx300086x.
Salihovic, S., Stubleski, J., Kärrman, A., Larsson, A., Fall, T., Lind, L., Lind, P.M., 2018. Changes in markers of liver function in relation to changes in perfluoroalkyl substances - a longitudinal study. Environ. Int. 117, 196–203. https://doi.org/10.1016/j.envint.2018.04.052.
Schymanski, E.L., Jeon, J., Gulde, R., Fenner, K., Ruff, M., Singer, H.P., Hollender, J., 2014. Identifying small molecules via high resolution mass spectrometry: communicating confidence. Environ. Sci. Technol. 48, 2097–2098. https://doi.org/10.1021/es5002105.
Sen, P., Qadri, S., Luukkonen, P.K., Ragnarsdottir, O., McGlinchey, A., Jäntti, S., Juuti, A., Arola, J., Schlezinger, J.J., Webster, T.F., Orešič, M., Yki-Järvinen, H., Hyötyläinen, T., 2022. Exposure to environmental contaminants is associated with altered hepatic lipid metabolism in non-alcoholic fatty liver disease. J. Hepatol. 76, 283–293. https://doi.org/10.1016/j.jhep.2021.09.039.
Stanifer, J.W., Stapleton, H.M., Souma, T., Wittmer, A., Zhao, X., Boulware, L.E., 2018. Perfluorinated chemicals as emerging environmental threats to kidney health: a scoping review. Clin. J. Am. Soc. Nephrol. 13, 1479–1492. https://doi.org/10.2215/CJN.04670418.
Tomczak, J.M., Weglarz-Tomczak, E., 2019. Estimating kinetic constants in the Michaelis – menten model from one enzymatic assay using Approximate Bayesian Computation. FEBS Lett. 593, 2742–2750. https://doi.org/10.1002/1873-3468.13531.
Tsaioun, K., Blaauboer, B.J., Hartung, T., 2016. Evidence-based absorption, distribution, metabolism, excretion (ADME) and its interplay with alternative toxicity methods. ALTEX 33, 343–358. https://doi.org/10.14573/altex.1610101.
United Nations Environment Programme, 2009. Decision SC-4/17. Listing of Perfluorooctane Sulfonic Acid, its Salts and Perfluorooctane Sulfonyl Fluoride.
United Nations Environment Programme, 2019. Decision: SC-9/12. Listing of Perfluorooctanoic Acid (PFOA), its Salts and PFOA-Related Compounds.
United Nations Environment Programme, 2022. Decision SC-10/13. Listing of Perfluorohexane Sulfonic Acid (PFHxS), its Salts and PFHxS-Related Compounds.
Van den Eede, N., Maho, W., Erratico, C., Neels, H., Covaci, A., 2013. First insights in the metabolism of phosphate flame retardants and plasticizers using human liver fractions. Toxicol. Lett. 223, 9–15. https://doi.org/10.1016/j.toxlet.2013.08.012.
Wang, Z., Dewitt, J.C., Higgins, C.P., Cousins, I.T., 2017. A never-ending story of per- and polyfluoroalkyl substances (PFASs)? Environ. Sci. Technol. 51, 2508–2518. https://doi.org/10.1021/acs.est.6b04806.
Wang, Z., Buser, A.M., Cousins, I.T., Demattio, S., Drost, W., Johansson, O., Ohno, K., Patlewicz, G., Richard, A.M., Walker, G.W., White, G.S., Leinala, E., 2021. A new OECD definition for per- and polyfluoroalkyl substances. Environ. Sci. Technol. 55, 15575–15578. https://doi.org/10.1021/acs.est.1c06896.
Wood, F.L., Houston, J.B., Hallifax, D., 2017. Clearance prediction methodology needs fundamental improvement: trends common to rat and human hepatocytes/microsomes and implications for experimental methodology. Drug Metab. Dispos. 45, 1178–1188. https://doi.org/10.1124/dmd.117.077040.
Zhou, Y., Oh, M.H., Kim, Y.J., Kim, E., Kang, J., Chung, S., Ju, C., Kim, W.-K., Lee, K., 2020. Metabolism and pharmacokinetics of SP-8356, a novel (1S)-(−)-Verbenone derivative, in rats and dogs and its implications in humans. Molecules 25, 1–14.
European Chemical Agency, 2020. Inclusion of Substances of Very High Concern in the Candidate List for Eventual Inclusion in Annex XIV. ECHA/01/2020.